ANL/XFD/CP-[illegible]

Submitted to the Specialists Meeting on Shielding Aspects of Accelerators, Targets and Irradiation Facilities, Knoxville, USA, September 1998.

Dose Measurements of Bremsstrahlung-Produced Neutrons from Thick Targets at the Advanced Photon Source

P.K. Job, M. Pisharody and E. Semones, Experimental Facilities Division, Argonne National Laboratories, 9700 S. Cass Ave., Argonne IL 60439, USA

Abstract

Bremsstrahlung is produced in the Advanced Photon Source storage ring when the positron beam interacts with the storage-ring components or with the residual gas molecules in the storage-ring vacuum. This bremsstrahlung has an energy range of zero to 7.0 GeV, which is the maximum energy of the positron beam. Bremsstrahlung photons of sufficiently high energy can interact with beamline components such as beam stops and collimators, generating neutrons of varying energies. This paper presents the results of simultaneous measurements, conducted at the Advanced Photon Source, of bremsstrahlung and the corresponding photoneutron production from thick targets of iron, copper, tungsten and lead, which allow one to correlate photoneutron dose rates from these metals as a function of bremsstrahlung power. The average photoneutron dose equivalent rates, normalized to the bremsstrahlung power, are measured as 2.7 ± 0.5 rem/h/W for iron, 3.2 ± 0.5 rem/h/W for copper, 3.9 ± 0.5 rem/h/W for tungsten, and 4.6 ± 0.8 rem/h/W for lead targets. These are measured at 80 cm lateral from the center of the targets, perpendicular to the photon beam direction.

Work supported in part by U.S. Department of Energy, Contract No. W-31-109-ENG-38, BES-Material Sciences, Argonne National Laboratory.

DISCLAIMER

Introduction

Bremsstrahlung is generated at the Advanced Photon Source (APS) storage ring by the radiative interaction of the circulating positron beam with both the residual gas molecules and the storage-ring components. Bremsstrahlung, produced along a typical 15.38-m straight path of the insertion device beamline of the APS, has been measured and analyzed in the previous studies [1,2]. The bremsstrahlung photons having sufficiently high energies (E_γ > 5.0 MeV), interacting with the beamline components like beam stops and collimators, can produce neutrons of varying energies by means of photonuclear interactions [3,4,5,6]. There are three processes by which photoneutrons may be produced by the high-energy bremsstrahlung photons: giant nuclear dipole resonance and decay (E_γ<40 MeV), quasi-deuteron production and decay (50<E_γ<300 MeV), and intranuclear cascade and evaporation (E_γ > 140 MeV). The giant resonance neutrons (GRN) are emitted almost isotropically and have an average energy of about 2 MeV. High-energy neutrons (E_n > 10 MeV) emitted from quasi-deuteron decay and intranuclear cascade are peaked in the forward direction. At the APS, where bremsstrahlung energy can be as high as 7 GeV, production of photoneutrons is possible from all the above processes although the fraction from giant resonance interaction dominates.

A simultaneous measurement of bremsstrahlung and the corresponding photoneutron production provides photoneutron dose rates as a function of bremsstrahlung power. Along with our bremsstrahlung spectrum measurements [1,2], we conducted simultaneous dose measurements at the APS from thick targets of iron (Fe), copper (Cu), tungsten (W) and lead (Pb) that are placed in the bremsstrahlung beam inside the first optics enclosure (FOE) of the insertion device beamlines. An Andersson-Braun remmeter, that houses a very sensitive pressurized ^{3}He detector, is used primarily for the giant resonance neutron dose equivalent rate measurements. The dose equivalent rates, normalized to bremsstrahlung power, beam current, and storage ring vacuum are measured for various targets.

Experimental Setup and Procedure

Four targets, Fe, Cu, W and Pb, each approximately 20 radiation lengths (X_0) long and 6 Moliere radii in the lateral dimension, are used for these measurements. The dimensions of the target have been chosen such that approximately 99% of the electromagnetic shower in both the longitudinal and the lateral directions are contained within the targets. The selection of the typical lateral dimension of the targets is also to minimize self-absorption of the generated giant resonance photoneutrons within the target. Only an approximately 6% reduction in dose equivalent rate is estimated in these target dimensions [7]. A complete description of the four targets used is summarized in Table 1.

A schematic of the combined bremsstrahlung-photoneutron experimental setup is shown in Figure 1. The target is placed inside the FOE of the beamline at about 170 cm from the beam exit window, aligned lengthwise along the photon beam. The lead-glass electromagnetic calorimeter, the central tube of which is also aligned along the photon beam, is placed approximately 40 cm behind the target. During bremsstrahlung measurements, the target is removed from the photon beam. The neutron dose equivalent rate measurements are made perpendicular to the incident photon beam direction. The Andersson-Braun (AB) remmeter is placed at a distance of about 80 cm at right angles to the aligned target, with the center of the remmeter aligned with the center of the target. The insertion device gap is kept in full open position to minimize the low-energy synchrotron radiation. A copper shield, which is about $0.5X_0$ thick, is placed in front of the lead-glass calorimeter to screen against the low-energy residual synchrotron radiation arriving at the FOE.

Experimental runs are conducted in such a way that each of the photoneutron measurement is preceded and followed by one bremsstrahlung measurement. Once the bremsstrahlung data set is collected, the target is placed in its marked position and the corresponding photoneutron data set is acquired. Then another bremsstrahlung data set is taken by removing the target. The average power from the two bremsstrahlung data sets is then used to normalize the photoneutron data. The changes in the beam current during this time is minimal due to the long particle beam life time in the storage ring and thus the measurements are approximately simultaneous.

Results and Discussion

The bremsstrahlung power and the corresponding photoneutron dose equivalent rates as a function of the beam current, measured 80 cm lateral from the targets, are given in Tables 2 and 3. The dose equivalent rates (DE) have been obtained from the net AB count rate using the calibration factors determined earlier. The errors shown on DE are statistical. The variation of neutron dose equivalent rate from each target as a function of the bremsstrahlung power is plotted in Figure 2 for the data given in Tables 2 and 3. The bremsstrahlung power plotted on the x-axis is an accurately measured quantity that relates to the actual storage ring vacuum and beam current variation. Thus, if the bremsstrahlung power is known, photoneutron dose equivalent rates from these four target materials can be normalized without having to rely on the storage ring parameters, like vacuum and beam current. The data from Figure 2, averaged over each target, is plotted in

Figure 3 as a function of the atomic number Z of the target material. The error on these average dose rates due to elemental impurities in the targets is less than 1%. It can be seen that the average bremsstrahlung normalized photoneutron dose equivalent rates, measured 80 cm perpendicular to the target center is 2.7 ± 0.5 rem/h/W for iron, 3.2 ± 0.5 rem/h/W for copper, 3.9 ± 0.5 rem/h/W for tungsten, and 4.6 ± 0.8 rem/h/W for lead targets.

The systematic corrections to the measured photoneutron dose equivalent (DE) rates should include thick target correction, correction due to wall-reflected neutrons, and a correction for the non-giant resonance neutron dose contribution. The thick target correction addresses the reduction in the giant resonance neutron fluence due to self absorption in the targets. With our target dimensions, calculations indicate a 6% reduction in the DE rates due to self absorption [7]. The neutrons produced could also reflect from the concrete ratchet wall close to the target (Figure 2) resulting in a net artificial increase in fluence. The AB response to this artificial increase in fluence depends upon its proximity to the reflecting wall and the nature of the neutron spectrum. Calculations estimate a 10% increase in DE rates detected by the AB remmeter due to neutron reflection. An estimation of the dose correction due to high-energy neutrons (non-GRN) requires the high-energy photoneutron neutron yield, corresponding dose conversion factors, and the AB remmeter detection efficiency to these neutrons. Calculations using PICA[8] gives a 12% reduction in the measured DE rates due to non-GRN neutrons. The final result of the above discussed corrections is an 8% net increase in the measured dose equivalent rates.

Comparison with Previous Results

Not many measurements of photoneutron dose equivalent rates have been conducted previously at energies as high as 7 GeV. Therefore, a true comparison of the present results with the existing ones is difficult. The existing results from earlier measurements are mostly either from low-energy incident electrons and photons [9,10] or from analytical relations and Monte Carlo simulations [11,12]. However, comparisons have been made with photoneutron dose equivalent rates from low-energy incident electrons deduced from the previous calculations [11]. These calculations do not take into account self-shielding effects. These results are also plotted in Figure 3 along with our measurements. The agreement is fairly good for tungsten and lead targets. For iron and copper targets the calculated values are smaller than the measurements.

The neutron dose equivalent rates from copper and tungsten, struck by bremsstrahlung produced from a 3-GeV electron storage ring are also discussed elsewhere [10]. These results are given normalized to storage ring vacuum and beam current. However an effort has been made to compare these results with our measurements from the beamline with the largest bremsstrahlung power. The comparison showed an order of magnitude difference in the photoneutron yield with our measurements. This is because the photoneutron dose rates normalized to beam current and vacuum may vary from beamline to beamline.

Conclusion

Photoneutron dose equivalent rates are measured as a function of bremsstrahlung power, from iron, copper, tungsten and lead thick targets placed in the bremsstrahlung beam at the insertion device beamlines of the Advanced Photon Source. The average photoneutron dose equivalent rates, normalized to the bremsstrahlung power, are measured as 2.7 ± 0.5 rem/h/W for iron, 3.2 ± 0.5 rem/h/W for copper, 3.9 ± 0.5 rem/h/W for tungsten, and 4.6 ± 0.8 rem/h/W for lead targets. These are measured at 80 cm lateral from the center of the targets, perpendicular to the photon beam direction. The measured photoneutron dose equivalent rates normalized to beam current and the storage ring vacuum vary from beamline to beamline because of the difference in the corresponding bremsstrahlung power.

References

[1] Pisharody, M., et al., Measurement of Gas Bremsstrahlung from the Insertion Device Beamlines of the APS, Argonne National Laboratory Report, ANL-APS-LS-260, (1997).

[2] Pisharody, M., et al., Measurement of Bremsstrahlung from the Electron Storage Rings, Nucl. Instr. Meth., A401, 442 (1997).

[3] Levinger, J.S., Theories of Photonuclear Reactions, Ann. Rev. Nucl. Sci.,4, 13 (1954).

[4] Strauch, K., Recent Studies of Photonuclear Reactions, Ann. Rev. Nucl. Sci., 2, 105 (1952).

[5] Levinger, J.S. and Bethe, H.A., Neutron Yield from Nuclear Photoeffect, Phy. Rev., 85, 577 (1952).

[6] Levinger, J.S., The High Energy Nuclear Photoeffect, Phy. Rev., 84, 43 (1951).

[7] Chapman, G.T. and Storrs, C.L., Effective Neutron Removal Cross Sections for Shielding, AECD-3978 (1955).

[8] Gabriel, T.A., et al., PICA -An Intranuclear Cascade Calculation for High Energy Photon Induced Nuclear Reactions, OakRidge National Laboratory Report, ORNL-4687 (1971).

[9] Barber, W.C. and George, W.D., Neutron Yields from Targets Bombarded by Electrons, Phy. Rev. 116, 1551 (1959).

[10] Liu, J.C.,et al., Gas Bremsstrahlung and Associated Photoneutron Shielding Calculations for the Electron Storage Rings, Health Phy. 68, 205 (1995).

[11] Swanson, W.P., Improved Calculation of the Photoneutron Yields Released by Incident Electrons, Health. Phy. 37, 347 (1979).

[12] Mao, X.S., et al., Giant Dipole Resonance Neutron Yields Produced by Electrons as a Function of Target Material and Thickness, Health Phy. 70, 207 (1996).

Table 1: Target dimensions and elemental purities.

Target Material	Length	Width	Elemental Purity
Fe	21.9 X_0 (38.4 cm)	5.9 X_m (9.6 cm)	93% Fe
Cu	19.5 X_0 (28.0 cm)	6.2 X_m (8.8 cm)	93% Cu
W	21.3 X_0 (8.0 cm)	6.1 X_m (6.0 cm)	95% W
Pb	20.5 X_0 (11.6 cm)	5.6 X_m (9.0 cm)	99% Pb

Table 2: Photoneutron dose equivalent rates at 80 cm lateral from target centers in beamline 11-ID.

Target Material	Beam Current I_b (mA)	Measured Vacuum P (nT)	Bremsstrahlung Power (kW)	Net AB Count Rate N_n (cps)	Neutron Dose Equivalent Rate DE (μrem/h)	Normalized Neutron Dose Equivalent Rate DE (μrem/h/kW)
Fe	96.6	9.26	1.66×10^{-8}	0.081	37.5±3.2	$(2.26\pm0.19)\times10^{9}$
Fe	93.3	8.95	1.72×10^{-8}	0.091	41.8±6.8	$(2.43\pm0.39)\times10^{9}$
Fe	90.2	8.70	1.63×10^{-8}	0.070	32.1±6.0	$(1.97\pm0.37)\times10^{9}$
Fe	81.2	8.04	1.24×10^{-8}	0.070	32.1±6.0	$(2.59\pm0.48)\times10^{9}$
Fe	80.3	7.96	1.20×10^{-8}	0.057	26.5±5.4	$(2.21\pm0.45)\times10^{9}$
Fe	72.5	7.23	8.96×10^{-9}	0.045	20.6±4.8	$(2.30\pm0.54)\times10^{9}$
Cu	96.0	9.20	1.81×10^{-8}	0.116	53.6±7.6	$(2.96\pm0.42)\times10^{9}$
Cu	93.2	8.92	1.68×10^{-8}	0.091	41.8±6.8	$(2.49\pm0.40)\times10^{9}$
Cu	87.3	8.51	1.48×10^{-8}	0.094	43.1±6.8	$(2.91\pm0.46)\times10^{9}$
Cu	83.2	8.12	1.28×10^{-8}	0.091	41.8±6.8	$(3.27\pm0.53)\times10^{9}$
Cu	77.5	7.71	1.14×10^{-8}	0.060	27.5±5.6	$(2.41\pm0.49)\times10^{9}$
W	88.3	8.64	1.53×10^{-8}	0.122	56.4±7.8	$(3.68\pm0.51)\times10^{9}$
W	87.9	8.56	1.58×10^{-8}	0.119	54.8±5.4	$(3.46\pm0.34)\times10^{9}$
W	79.5	7.82	1.18×10^{-8}	0.082	38.0±6.4	$(3.22\pm0.54)\times10^{9}$
W	79.2	7.90	$1\ 10\times10^{-8}$	0.081	37.4±3.2	$(3.40\pm0.29)\times10^{9}$
W	76.5	7.61	1.07×10^{-8}	0.092	42.4±6.8	$(3.95\pm0.63)\times10^{9}$
Pb	90.9	8.87	1.62×10^{-8}	0.129	59.5±8.0	$(3.67\pm0.49)\times10^{9}$
Pb	79.4	7.79	1.20×10^{-8}	0.099	45.7±7.0	$(3.79\pm0.58)\times10^{9}$
Pb	78.5	7.76	1.12×10^{-8}	0.099	45.7±7.0	$(4.08\pm0.62)\times10^{9}$
Pb	70.8	7.08	8.96×10^{-9}	0.079	36.2±6.2	$(4.04\pm0.69)\times10^{9}$

Table 3: Photoneutron dose equivalent rates at 80 cm lateral from target centers in beamline 6-ID.

Target Material and Detector	Beam Current I_b (mA)	Measured Vacuum P (nT)	Bremsstrahlung Power (kW)	Net AB Count Rate N_n (cps)	Neutron Dose Equivalent Rate DE (μrem/h)	Normalized Neutron Dose Equivalent Rate DE (μ rem/h/kW)
Fe,BF_3	93.4	9.77	5.31×10^{-9}	0.033	15.4±3.0	$(2.90\pm0.56)\times10^{9}$
Fe,BF_3	92.7	9.62	5.06×10^{-9}	0.031	14.5±2.8	$(2.87\pm0.55)\times10^{9}$
Fe,^{3}He	89.1	9.27	4.93×10^{-9}	0.102	12.9±1.4	$(2.61\pm0.28)\times10^{9}$
Fe,BF_3	78.2	8.41	3.71×10^{-9}	0.026	11.8±2.6	$(3.18\pm0.70)\times10^{9}$
Cu,^{3}He	90.3	9.44	4.10×10^{-9}	0.081	10.3±1.2	$(2.06\pm0.24)\times10^{9}$
Cu,BF_3	89.9	9.37	4.88×10^{-9}	0.034	15.7±3.0	$(3.20\pm0.61)\times10^{9}$
Cu,BF_3	81.1	8.59	4.09×10^{-9}	0.028	13.1±1.8	$(3.21\pm0.44)\times10^{9}$
Cu,BF_3	62.9	7.02	2.43×10^{-9}	0.018	8.5±2.2	$(3.50\pm0.91)\times10^{9}$
W,^{3}He	90.0	9.38	5.06×10^{-9}	0.139	17.7±1.6	$(3.49\pm0.32)\times10^{9}$
W,BF_3	87.0	9.19	4.64×10^{-9}	0.042	19.4±3.2	$(4.17\pm0.69)\times10^{9}$
W,^{3}He	85.7	9.10	4.63×10^{-9}	0.107	13.5±1.4	$(2.92\pm0.30)\times10^{9}$
W,BF_3	82.3	8.76	4.19×10^{-9}	0.034	15.5±3.0	$(3.71\pm0.72)\times10^{9}$
W,^{3}He	77.7	8.30	3.61×10^{-9}	0.111	14.0±1.0	$(3.89\pm0.28)\times10^{9}$
Pb,BF_3	76.1	8.22	3.55×10^{-9}	0.038	17.7±3.2	$(4.98\pm0.90)\times10^{9}$
Pb,BF_3	63.9	7.12	2.54×10^{-9}	0.027	12.3±2.6	$(4.84\pm1.02)\times10^{9}$

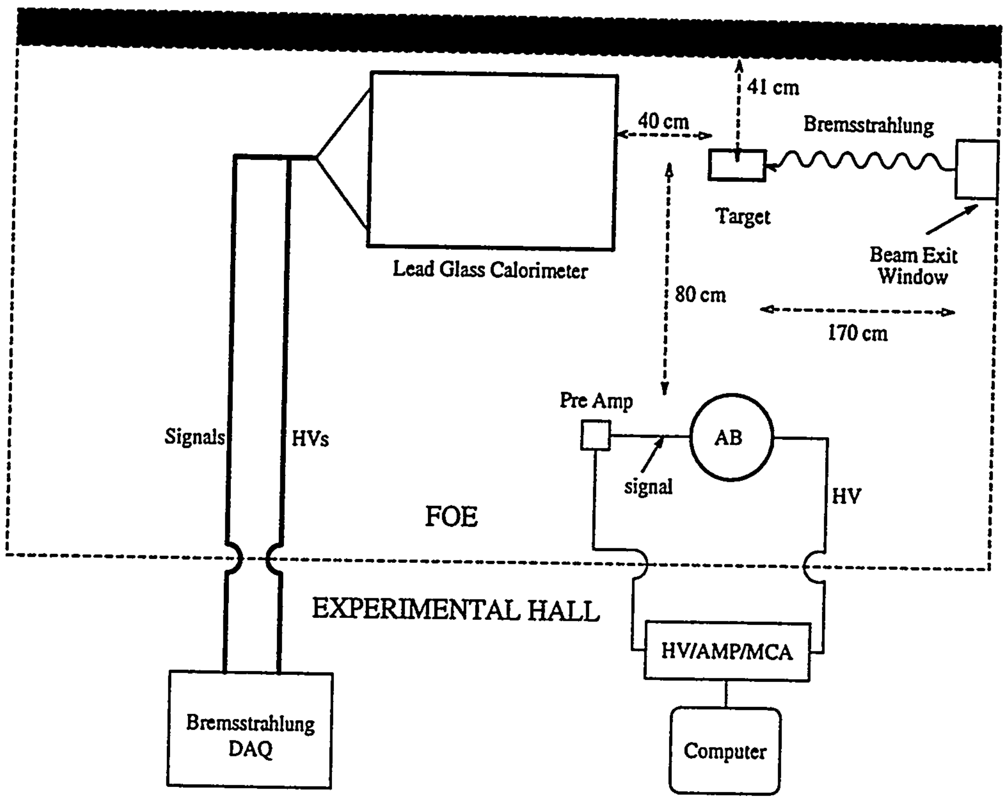

Figure 1: Schematic of the top view of the Andersson-Braun remmeter and the calorimeter along with the associated data acquisition systems that measure the photoneutron dose equivalent rates and the bremsstrahlung power.

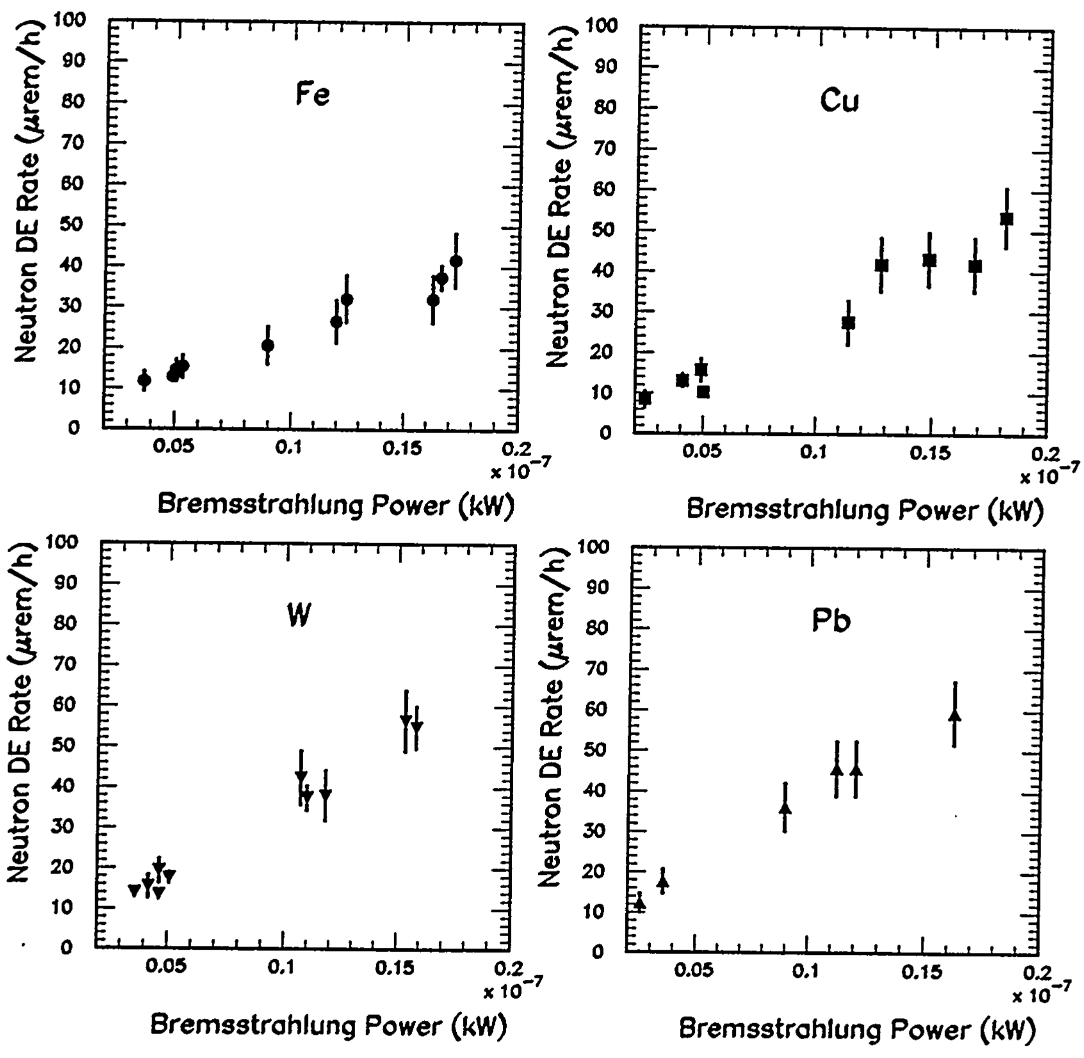

Figure 2: The photoneutron dose equivalent rate, measured 80 cm lateral from each target center, as a function of the incident bremsstrahlung power.

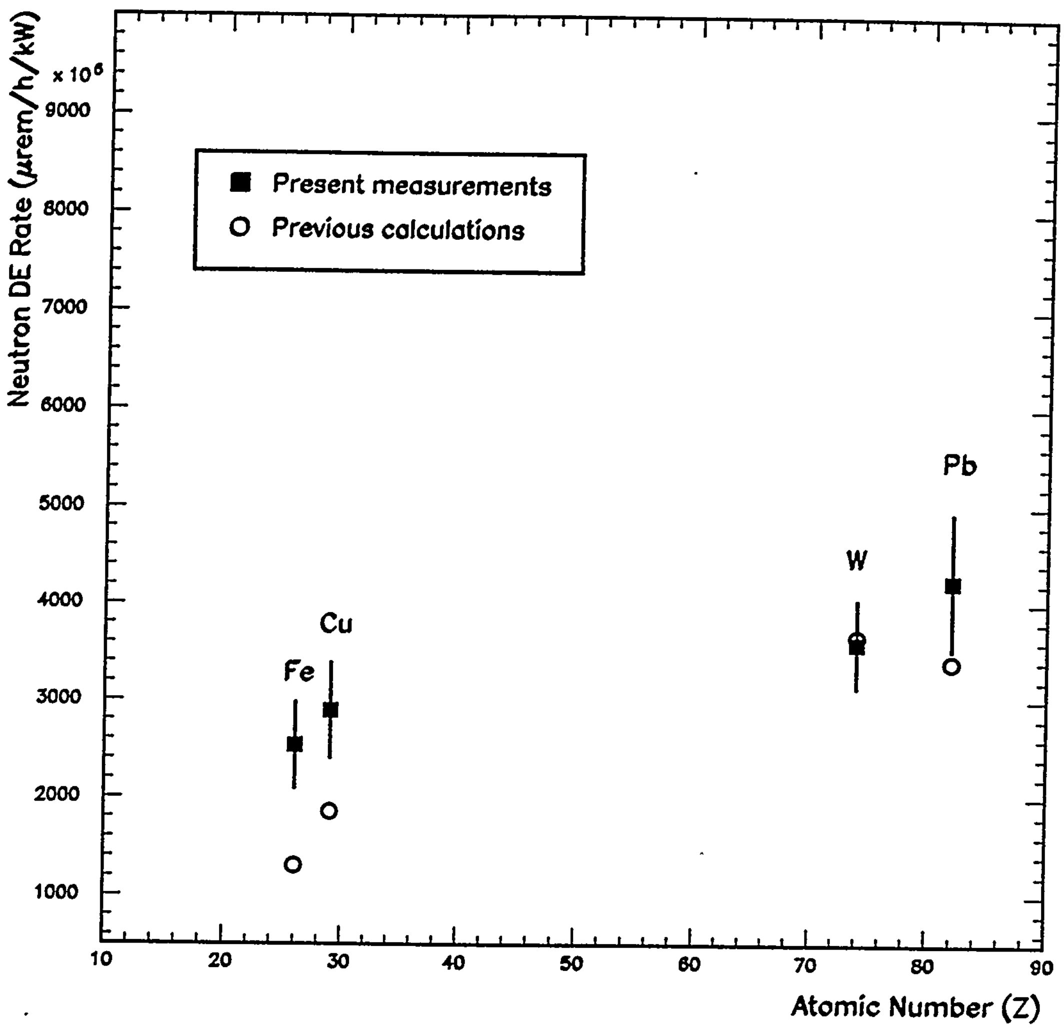

Figure 3: The photoneutron dose equivalent rate at 80 cm perpendicular to each of the target center, normalized to the incident power, shown plotted as a function of the atomic number. The present measurements are the average of all the data from both beamlines 11 ID and 6 ID. The results deduced from previous calculations of photoneutron yields released by incident electrons [11] are also shown for comparison.